DALTON
FULL PAPER

# New molybdenum(v) analogues of Amavadin and their redox properties

**Paul D. Smith,[a] J. Jon A. Cooney,[a] Eric J. L. McInnes,[b] Roy L. Beddoes,[a] David Collison,*[a] Spencer M. Harben,[a] Madeleine Helliwell,[a] Frank E. Mabbs,[b] Alexander Mandel,[c] Annie K. Powell[c] and C. David Garner*[d]**

[a] *Department of Chemistry, The University of Manchester, Oxford Road, Manchester, UK M13 9PL. E-mail: david.collison@manchester.ac.uk*
[b] *EPSRC CW EPR Service Centre, Department of Chemistry, The University of Manchester, Oxford Road, Manchester, UK M13 9PL*
[c] *School of Chemical Sciences, The University of East Anglia, Norwich, UK NR4 7TJ*
[d] *School of Chemistry, The University of Nottingham, University Park, Nottingham, UK NR2 2RD*

***Received 19th March 2001, Accepted 11th July 2001***
***First published as an Advance Article on the web 27th September 2001***

Reactions of $[MoO_2(acetylacetonate)_2]$ with the proligands (*N*-hydroxyimino)diacetic acid ($H_3$hidpa), *R*,*R*-2,2′-(*N*-hydroxyimino)dipropionic acid (*R*,*R*-$H_3$hidpa) or *R*,*S*-2,2′-(*N*-hydroxyimino)dibutyric acid (*R*,*S*-$H_3$hidba) yielded the compounds $[PPh_4][\Delta,\Lambda\text{-Mo(hida)}_2]\cdot CH_2Cl_2$ **1**, $[H_5O_2][\Delta\text{-Mo}(R,R\text{-hidpa})_2]$ **2**, $[PPh_4][\text{Mo}(R,S\text{-hidba})_2]\cdot 2H_2O$ **3a** and $Na[\Delta,\Lambda\text{-Mo}(R,S\text{-hidba})_2]\cdot{}^1\!/_4{}^i\!Pr_2O$ **3b**, respectively. Reactions of $H_3$hida with a methanolic solution of $[PPh_4][MoOCl_4(H_2O)]$ in the presence of NaOH (*ca.* pH 8) provided an alternative synthesis for **1**. The complex of **1** when transferred into $CH_2Cl_2$ using $[PPh_4]Br$ yielded brown block-like crystals from a $CH_2Cl_2$–EtOH solution, however, **2** and **3b** were crystallised from $H_2O$ and MeCN solutions with $[H_5O_2]^+$ and $[Na]^+$ counter cations, respectively. X-Ray crystallography confirmed the same distinctive eight-co-ordinate geometry of the complex anions of **1**, **2** and **3b** as identified for Amavadin, the form in which vanadium(IV) is bound in *Amanita muscaria* mushrooms. EPR and UV/vis spectra recorded for **1**, **2** and **3a** are consistent with the presence of molybdenum(V). Cyclic voltammetric studies using a glassy carbon working electrode in $CH_2Cl_2$ for **1** exhibited a reversible $Mo^{VI}/Mo^{V}$ and a quasi-reversible $Mo^{V}/Mo^{IV}$ redox couple at $E_{1/2} = +0.96$ and $-0.99$ V (*vs.* a saturated calomel electrode), respectively. Complex **3a** also displayed a reversible $Mo^{VI}/Mo^{V}$ redox couple at $E_{1/2} = +0.77$ V, whereas the $Mo^{V}/Mo^{IV}$ couple was irreversible ($E_{pc} = -1.28$ V). Additional electrochemical studies with **2** recorded a reversible $Mo^{VI}/Mo^{V}$ redox couple in $Me_2SO$ ($E_{1/2} = +0.77$ V), however in $H_2O$ this one-electron oxidation process is irreversible.

## Introduction

Mushrooms of the genus *Amanita* accumulate vanadium to concentrations of up to 400 mg $kg^{-1}$ (dry weight)[1] in the form of the discrete moiety Amavadin,[2] a 1 : 2 complex of vanadium(IV) with the proligand *S*,*S*-*N*-hydroxyiminodipropionic acid (*S*,*S*-$H_3$hidpa = $HON\{CH(CH_3)CO_2H\}_2$).[3–5] The presence of $V^{IV}$ is clearly indicated by EPR spectroscopy[6] and the metal centre can be reversibly oxidised to the $V^{V}$ level.[7] Thus this species belongs to the group of transition metal centres in biology which exhibit reversible, one-electron, redox behaviour. This redox behaviour may account for the biological role of Amavadin and, in solution, has been shown to mediate the oxidation of glutathione and other biologically active thiols.[8,9] Recent studies[5,10,11] into the chemical nature of Amavadin have established a novel eight-co-ordinate geometry, with each *S*,*S*-$H_3$hidpa proligand co-ordinated *via* an $\eta^2$-NO group and two unidentate carboxylate groups. Complementary work[10,12,13] has included the analogues from *N*-hydroxyiminodiacetic acid ($H_3$hida = $HON\{CH_2CO_2H\}_2$) which provide further examples of this distinctive eight-co-ordinate structure. This co-ordination environment leads to chirality at the vanadium (Scheme 1) and the isolated natural product Amavadin consists of an approximately equimolar mixture of the Δ- and Λ-helical forms of $[V(S,S\text{-hidpa})_2]^{2-}$.[10,11] These complexes are assigned idealised $C_2$ point symmetry in solution, where the two-fold axis bisects angles between the normals to the {VNO} plane from each ligand projected through the metal atom. The special co-ordination geometry and chemical behaviour of Amavadin has generated curiosity as to whether it is possible to extend this chemistry to other metals. Therefore, studies of the reactivity of $H_3$hidpa towards other metal centres, especially those found in biological systems, were initiated. The synthesis and characterisation of $[PPh_4][\Delta\text{-Mo}(R,R\text{-hidpa})(R,S\text{-hidpa})]$ and its enantiomer,[14] that involve molybdenum(V) bound to two mutually *trans* $\eta^2$-NO groups and four unidentate carboxylates, was the first example of a chemical analogue of Amavadin. This complex is capable of both a one-electron reversible oxidation and a one-electron reversible reduction in $CH_2Cl_2$. Other developments, notably studies of $[M(hidca)_2]^{-/2-}$ ($H_3$hidca = *N*-hydroxyiminodicarboxylic acid, $HON\{CH(R)CO_2H\}_2$, for R = alkyl) have been reported,[15] and the chemistry described herein has led to several new molybdenum complexes related to Amavadin.

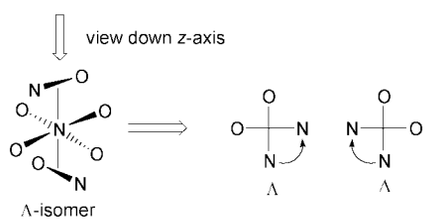


**Scheme 1** Isomerism at the vanadium centre.

 DOI: 10.1039/b102531g

## Experimental

### Reagents and apparatus

All reagent and solvents were obtained from normal commercial sources and were used without further purification unless otherwise stated. Tetrahydrofuran (thf) and $Et_2O$ were distilled from sodium; $CH_2Cl_2$ and MeCN were distilled from $CaH_2$, and all solvents were stored under dinitrogen. The proligands $H_3$hida and *R*,*R*-$H_3$hidpa were synthesised using a modification of the method [16] described by Felcman *et al.*,[17] and purification was carried out using the procedure outlined by Koch *et al.*[18] *R*,*S*-$H_3$hidba (*R*,*S*-*N*-hydroxyiminodibutyric acid = HON{$CH(C_2H_5)CO_2H$}$_2$) was synthesised as described by Smith *et al.*[15] [$MoO_2$(acetylacetonate)$_2$] was synthesised as described by Jones,[19] by treatment of an aqueous solution of $Na_2[MoO_4]$ with HCl (*ca.* pH 1) and acetylacetone to produce a yellow precipitate. [$PPh_4$][$MoOCl_4(H_2O)$] was prepared as a green crystalline product from a solution of [$MoCl_5$] in conc. HCl in the presence of [$PPh_4$]Cl.[20] Chemical analyses were performed by The University of Manchester, Microanalytical Laboratory. IR spectra were recorded on a Perkin-Elmer 1710 FT spectrometer. Electronic absorption spectra were recorded on a Varian Cary 1E UV/vis spectrophotometer. Mass spectra were recorded using a KRATOS concept 1S spectrometer (matrix NBA). X-Band (*ca.* 9.5 GHz) EPR spectra were recorded on a Bruker ESP300E spectrometer.

Electrochemical measurements were made with a PAR model 175 waveform generator, a model 173 potentiostat, and a PAR electrochemistry cell with a three-electrode configuration consisting of a glassy carbon working electrode, a saturated calomel reference electrode (SCE) and a platinum wire secondary electrode. Data were recorded on an Advance Bryans Series 6000 XY/t recorder. The cyclic voltammograms were recorded for solutions of compound (*ca.* 1 mmol $dm^{-3}$) with [$NBu^n_4$][$BF_4$] (*ca.* 0.2 mol $dm^{-3}$) as supporting electrolyte in non-aqueous media, prepared from Na[$BF_4$] and [$NBu^n_4$][$HSO_3$] and recrystallised from toluene.[21] KCl (*ca.* 0.2 mol $dm^{-3}$) was used as supporting electrolyte for cyclic voltammograms recorded in $H_2O$. Controlled potential electrolysis (CPE) experiments were carried out in a two-compartment cell separated by Vycor porous glass. The working electrode consisted of a cube of reticulated vitreous carbon, purchased from The Electrosynthesis Co, Inc., Lancaster, NY 14086, and the secondary electrode was platinum mesh. All solutions were deoxygenated by bubbling dinitrogen through them for several minutes prior to use and all voltammograms were recorded with solutions under a dinitrogen atmosphere at 293 K. An optically transparent thin layer electrode (OTTLE) was supported in a cell and poly(tetrafluoroethylene) block from the design developed by Heath *et al.*[22] All electrochemical potentials were measured relative to SCE and were corrected for liquid-junction potentials in non-aqueous media *via* the use of the ferrocenium–ferrocene couple as an internal redox standard ([$(Cp)_2Fe]^+$/[$(Cp)_2$Fe]; $\Delta E$ = 65 mV, $i_{pa} : i_{pc} = 0.96$).[23]

### Syntheses

**[$PPh_4$][Δ,Λ-Mo(hida)$_2$]·$CH_2Cl_2$ 1.** *Method 1.* [$MoO_2$(acetylacetonate)$_2$] (326 mg, 1.00 mmol) was added to a solution of $H_3$hida (315 mg, 2.10 mmol) in $H_2O$ (10 $cm^3$). The reaction mixture was stirred (*ca.* 3 h) at 323 K, whereupon a dark brown–purple solution formed. After cooling (to *ca.* 293 K), a solution of [$PPh_4$]Br (419 mg, 1.00 mmol) in $CH_2Cl_2$ (10 $cm^3$) was mixed with the aqueous phase and after rapid stirring (for *ca.* 30 min) the dark brown–purple colour transferred into the $CH_2Cl_2$ layer. The $CH_2Cl_2$ phase was separated from the aqueous layer and dried over anhydrous $CaCl_2$ (for *ca.* 1 h), filtered and then EtOH (10 $cm^3$) was added. Brown–purple block-like crystals were obtained by slow evaporation (*ca.* 48 h) at 293 K from the resulting solution, and these were collected and dried under vacuum. Yield, 380 mg, 47% (Found: C, 48.74; H, 3.78; N, 3.54; Mo, 11.65; P, 3.9%. Calc. for $C_{33}H_{30}N_2O_{10}Cl_2MoP$: C, 48.71; H, 3.72; N, 3.44; Mo, 12.04; P, 3.81%). IR (KBr, $cm^{-1}$): 1690 [ν(C=O)], 1353 [ν(C–O)], 1108 [ν(N–O)]. UV/Vis (MeCN): ν/$cm^{-1}$ (ε/$mol^{-1}$ $dm^3$ $cm^{-1}$) 26455 (103) and 18181 (19). Mass spectrum (negative-ion FAB): *m*/*z* 390 = [Mo(hida)$_2$]$^-$.

*Method 2.* [$PPh_4$][$MoOCl_4(H_2O)$] (611 mg, 1.00 mmol) was dissolved in acetone (15 $cm^3$) and dinitrogen bubbled through the solution. $H_3$hida (315 mg, 2.10 mmol) was dissolved in MeOH (6 $cm^3$) and the pH (as measured by Whatman paper 3 pH 1–11 colour indicator paper) adjusted to 8 with NaOH (5 mol $dm^{-3}$). On addition of the $H_3$hida solution to that of [$PPh_4$][$MoOCl_4(H_2O)$] an instant colour change occurred and a brown precipitate formed. The reaction mixture was stirred (for *ca.* 10 min) and then the solvent removed under vacuum. The resulting residue was extracted into $CH_2Cl_2$ (10 $cm^3$), dried over anhydrous $CaCl_2$ (for *ca.* 1 h) and crystals were obtained from this solution as described in Method 1. Yield, 350 mg, 43% (Found: C, 48.12; H, 3.66; N, 3.38%. Calc. for $C_{33}H_{30}N_2O_{10}Cl_2MoP$: C, 48.71; H, 3.72; N, 3.44%).

**[$H_5O_2$][Δ-Mo(*R*,*R*-hidpa)$_2$] 2.** [$MoO_2$(acetylacetonate)$_2$] (326 mg, 1.00 mmol) was added to a solution of *R*,*R*-$H_3$hidpa (431 mg, 2.10 mmol) in $H_2O$ (10 $cm^3$). The reaction mixture was stirred (for *ca.* 3 h) at 323 K, whereupon a brown solution formed, which was allowed to cool (to *ca.* 293 K) and was filtered. This solution was concentrated by evaporation under vacuum (2 $cm^3$) and cooled (to *ca.* 273 K) then added to cold (*ca.* 273 K) thf (20 $cm^3$) and a brown precipitate formed that was collected and dried under vacuum. Brown block-like crystals suitable for X-ray diffraction were obtained by slow evaporation of an aqueous solution of the precipitate at 293 K. Yield, 240 mg, 52% (Found: C, 30.4; H, 4.27; N, 5.78; Mo, 21.67%. Calc. for $C_{12}H_{21}N_2O_{12}Mo$: C, 29.81; H, 4.38; N, 5.8; Mo, 20.27%). IR (KBr, $cm^{-1}$): 1650 [ν(C=O)], 1366 [ν(C–O)], 1121 [ν(N–O)]. UV/Vis ($H_2O$): ν/$cm^{-1}$ (ε/$mol^{-1}$ $dm^3$ $cm^{-1}$) 26041 (61) and 18181 (15). Mass spectrum (negative-ion FAB): *m*/*z* 444 = [Mo(hidpa)$_2$]$^-$.

**[$PPh_4$][Mo(*R*,*S*-hidba)$_2$]·$2H_2O$ 3a.** [$MoO_2$(acetylacetonate)$_2$] (326 mg, 1.00 mmol) was added to a solution of *R*,*S*-$H_3$hidba (431 mg, 2.1 mmol) in MeOH (10 $cm^3$) and the reaction mixture was stirred (for *ca.* 18 h) at 293 K, whereupon a brown solution formed. [$PPh_4$]Br (419 mg, 1.00 mmol) was added and the solution evaporated to dryness under vacuum. The resulting residue was extracted into thf (10 $cm^3$) and filtered to remove any excess [$PPh_4$]Br. This solution was cooled (to 275 K) and added dropwise into cold (275 K) $Et_2O$ (50 $cm^3$) and produced a brown precipitate. The solid product was very hygroscopic and therefore was collected in a dinitrogen atmosphere, washed with $Et_2O$ (10 $cm^3$), dried under vacuum and stored under dinitrogen over silica-gel. Yield, 605 mg, 72% (Found: C, 53.75; H, 5.19; N, 3.17; Mo, 10.80; P, 3.28%. Calc. for $C_{40}H_{48}N_2O_{12}MoP$: C, 54.72; H, 5.51; N, 3.19; Mo, 11.16; P, 3.53%). IR (KBr, $cm^{-1}$): 1675 [ν(C=O)], 1459 [ν(C–O)], 1131 [ν(N–O)]. UV/Vis (MeCN): ν/$cm^{-1}$ (ε/$mol^{-1}$ $dm^3$ $cm^{-1}$) 26595 (94) and 17730 (10). Mass spectrum (negative-ion FAB): *m*/*z* 502 = [Mo(hidba)$_2$]$^-$.

**Na[Δ,Λ-Mo(*R*,*S*-hidba)$_2$]·¼$^i$$Pr_2O$ 3b.** [$MoO_2$(acetylacetonate)$_2$] (326 mg, 1.00 mmol) was added to a solution of *R*,*S*-$H_3$hidba (431 mg, 2.10 mmol) in MeOH (10 $cm^3$), previously treated with NaOH (40 mg, 1.0 mmol). This reaction mixture was stirred (for *ca.* 18 h) at 293 K, whereupon a brown solution formed and was evaporated to dryness under reduced pressure. The resulting residue was extracted into MeCN (10 $cm^3$) and red block-like crystals suitable for X-ray diffraction were obtained from this solution *via* the slow vapour diffusion technique using $^i$$Pr_2O$ at 273 K. Yield, 285 mg, 51% (Found: C, 34.81; H, 5.17; N, 5.07; Mo, 17.77; Na, 4.17%. Calc. for $C_{16}H_{24}N_2O_{10}MoNa·2H_2O$: C, 34.35; H, 5.01; N, 5.00; Mo, 17.17; Na,

**Table 1** Crystal data for compounds **1**, **2** and **3b**

| | | | |
|---|---|---|---|
| Empirical formula | $C_{33}H_{30}Cl_2MoN_2O_{10}P$ (**1**) | $C_{12}H_{21}MoN_2O_{12}$ (**2**) | $C_{39}H_{55}N_4O_{20.5}Mo_2Na_2$ (**3b**) |
| Formula weight | 812.43 | 481.25 | 547.32 |
| Crystal colour, habit | Brown, block | Brown, block | Red, block |
| Crystal dimensions/mm | 0.20 × 0.25 × 0.35 | 0.8 × 0.3 × 0.3 | 0.17 × 0.17 × 0.25 |
| Crystal system | Monoclinic | Orthorhombic | Orthorhombic |
| *a*/Å | 7.96(1) | 10.3610(10) | 28.23(1) |
| *b*/Å | 28.043(6) | 13.9210(10) | 30.29(1) |
| *c*/Å | 15.47(1) | 6.8470(10) | 11.64(1) |
| *β*/° | 91.54(8) | — | — |
| *V*/Å$^3$ | 3451(5) | 987.6(2) | 9956(17) |
| Space group | $P2_1/c$ (no. 14) | $P2_12_12$ (no. 18) | *Fddd* (no. 70) |
| *Z* | 4 | 2 | 16 |
| $D_{calc}$/g cm$^{-3}$ | 1.564 | 1.618 | 1.460 |
| $\mu$/cm$^{-1}$ | Cu-Kα, 55.76 | Mo-Kα, 7.25 | Cu-Kα, 49.33 |
| Diffractometer | Rigaku AFC5R | Rigaku AFC7R | Rigaku AFC5R |
| *λ*/Å | 1.54178 | 0.71073 | 1.54178 |
| *T*/K | 296 ± 1 | 293 ± 2 | 293 ± 1 |
| Scan type | *ω*–2*θ* | *ω* | *ω*–2*θ* |
| $2\theta_{max}$/° | 120.1 | 60 | 158.9 |
| No. of reflections measured | Total: 5679<br>Unique: 5257<br>($R_{int}$ = 0.046) | Total: 1674<br>Unique: 1674<br>($R_{int}$ = 0.0) | Total:2857<br>Unique: 2857 |
| Corrections | Lorentz-polarisation<br>Absorption (DIFABS)[24] | Lorentz-polarisation | Lorentz-polarisation<br>Absorption (*ψ*-scans) |
| No. of observations | 3765 [$I > 3.00\sigma(I)$] | 1674 [$I > 2.00\sigma(I)$] | 1583 [$I > 2.00\sigma(I)$] |
| No. of variables | 442 | 125 | 155 |
| Residuals | $R$ = 0.098; $R_w$ = 0.130 | $R$ = 0.0279; $R_w$ = 0.0749 [$I > 2\sigma(I)$]<br>$R$ = 0.0297; $R_w$ = 0.0760 (all data) | $R$ = 0.064; $R_w$ = 0.053 |
| Goodness of fit indicator | 3.58 | 1.088 | 1.94 |

4.11%). UV/Vis ($H_2O$): $\nu$/cm$^{-1}$ ($\varepsilon$/mol$^{-1}$ dm$^3$ cm$^{-1}$) 24943 (60) and 17841 (13). Mass spectrum (negative-ion FAB): *m*/*z* 502 = $[Mo(hidba)_2]^-$.

### X-Ray crystallography

A summary of the crystallographic information obtained for **1**, **2** and **3b** is provided in Table 1. The structures were solved by direct methods using SIR[24,25a] for **1** and SHELXS[25a] for **2** and **3b**. Non-hydrogen atoms were refined anisotropically. Hydrogen atoms were included in the structure factor calculations[26] in idealised positions (C–H = 0.95 Å) and were assigned isotropic thermal parameters that were 20% greater than the equivalent *B* value of the atom to which they were bonded. For **1** and **3b** all calculations were performed using the TEXSAN[27a] crystallographic software package. For **2** the data were refined against $F^2$ using SHELXL93.[27b]

CCDC reference numbers 168519–168521.

See http://www.rsc.org/suppdata/dt/b1/b102531g/ for crystallographic data in CIF or other electronic format.

## Results and discussion

The values for the Mo analysis are reasonably close to the expected values, however the C, H, N, Na and P are closer and the spectral and crystallographic data are consistent with the formulae given.

### Crystallography

After the initial investigation with vanadium[5,10–13] and recent results with molybdenum,[14] herein we report the structures of further examples of molybdenum(v) analogues of Amavadin. **1** forms brown block-like crystals in the space group $P2_1/c$ (no. 14) (Table 1). As expected, the complex anion exhibits the eight-co-ordinate geometry found in Amavadin containing a 1 : 2 complex of molybdenum(v) with $hida^{3-}$, bound by two mutually *trans* $\eta^2$-NO groups and four unidentate carboxylates, see Fig. 1. The asymmetric unit contains half the complex anion and a $[PPh_4]^+$ counter cation with a molecule of $CH_2Cl_2$. The anion was refined as the Δ-helical form at the molybdenum(v) centre. The space group has a centre of symmetry; therefore the equivalent Λ-isomer at the metal centre is generated in the unit cell. The Mo–O and Mo–N bond lengths are similar to those in [Δ-Mo(*R*,*R*-hidpa)(*R*,*S*-hidpa)]$^-$[14] (Table 2), and are each slightly longer (range 0.13–0.02 Å; av. 0.07 Å) than their counterparts in $[V(hida)_2]^-$.[10] The planes of the two {MoNO} groups are perpendicular (90.04°, as measured from N to O, see Scheme 1) and each is effectively perpendicular (88.92; 90.49°) to the least-squares plane of the molybdenum and the four-co-ordinated carboxylate oxygen atoms (the "equatorial" plane). These oxygen atoms are significantly displaced from this least-squares plane; O(1) and O(5) sit below (−0.42 and −0.38 Å, respectively) and O(6) and O(10) sit above (0.36 and 0.39 Å, respectively) the plane, which contains the molybdenum.

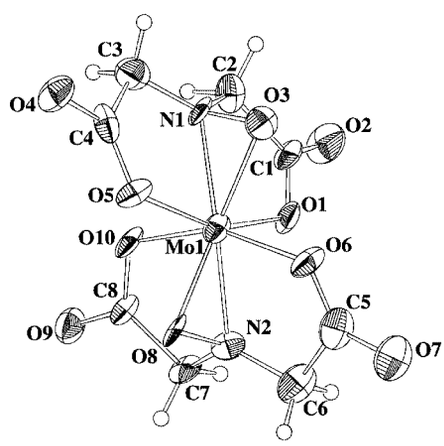


**Fig. 1** ORTEP[39] representation of the structure of the anion present in **1**.

Initial reactions of $[PPh_4][MoOCl_4(H_2O)]$ with $H_3$hidpa resulated in fragmentation of the proligand and yielded a product which contained a novel 2-(oxyimino)propionic acid moiety, $[PPh_4][MoO_2Cl_2(NOC(Me)CO_2H)]$.[28] X-Ray crystallography showed that the molybdenum(VI) was bound to two oxo groups, two chlorides, and the $[NOC(Me)CO_2H]$ fragment co-ordinated *via* the nitrogen and an oxygen atom in the $\{CO_2H\}$ group. However, when this reaction was repeated under basic conditions (see Experimental section), facile chloride abstraction was promoted and the eight-co-ordinate

**Table 2** Comparison of selected bond lengths (Å) and angles (°) for **1**, **2**, **3b** and $[PPh_4][Mo(R,R\text{-hidpa})(R,S\text{-hidpa})]$ [14]

| | **1** | **2**[a,b] | **3b**[a] | $[PPh_4][\Delta\text{-}Mo(R,R\text{-hidpa})(R,S\text{-hidpa})]$ |
|---|---|---|---|---|
| Mo(1)–O(1) | 2.01(1) | 2.064(2) | 2.053(6) | 2.050(7) |
| Mo(1)–O(5) | 2.04(1) | 2.062(2) | 2.039(6) | 2.066(7) |
| Mo(1)–O(6) | 2.038(9) | 2.064(2) | 2.053(6) | 2.017(9) |
| Mo(1)–O(10) | 2.074(9) | 2.062(2) | 2.039(6) | 1.99(1) |
| Mo(1)–O(3) | 2.01(1) | 2.002(2) | 2.003(6) | 2.001(8) |
| Mo(1)–O(8) | 2.00(1) | 2.002(2) | 2.003(6) | 2.003(7) |
| Mo(1)–N(1) | 2.09(1) | 2.070(2) | 2.101(7) | 2.055(8) |
| Mo(1)–N(2) | 2.09(1) | 2.070(2) | 2.101(7) | 2.054(9) |
| N(1)–O(3) | 1.41(1) | 1.394(3) | 1.406(7) | 1.36(1) |
| N(2)–O(8) | 1.46(1) | 1.394(3) | 1.406(7) | 1.39(1) |
| N(1)–Mo(1)–O(1) | 40.0(4) | 39.99(9) | 40.0(2) | 39.1(3) |
| N(2)–Mo(1)–O(8) | 41.9(4) | 39.99(9) | 40.0(2) | 40.1(3) |

[a] $C_2$ symmetry at the molybdenum centre, hence N(2), O(6), O(8), and O(10) are generated by symmetry. O(1,5,6,10) are carboxylate O atoms and O(3,8) are the $\eta^2$-NO O atoms. [b] O(3) and O(5) renumbered for comparison.

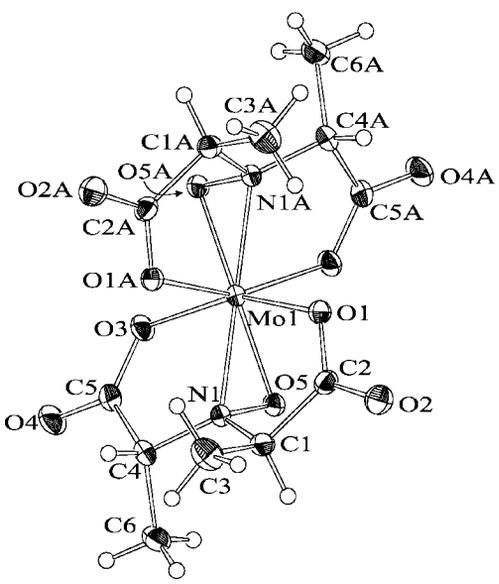


**Fig. 2** ORTEP representation of the structure of the anion present in **2**.

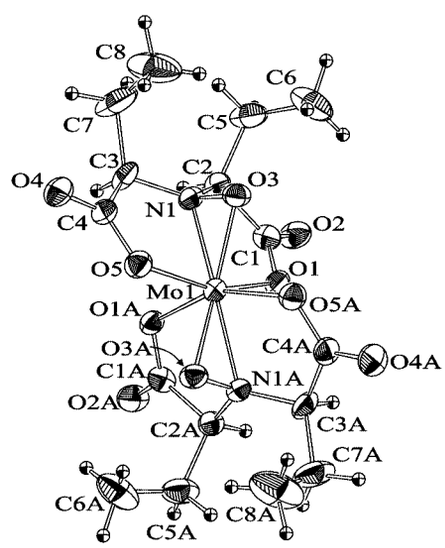


**Fig. 3** ORTEP representation of the structure of the anion present in **3b**.

Amavadin-style complex was isolated, providing a rapid and alternative synthesis of **1**.

**2** crystallised as brown blocks in the space group $P2_12_12$ (no. 18) (Table 1). The complex anion exhibits the eight-co-ordinate geometry found in Amavadin, see Fig. 2. The asymmetric unit consists of half the complex anion with the Δ-form at the molybdenum(v) centre plus an oxygen atom (O6) around which three peaks were observed in the final difference map. These can be assigned to two full occupancy H atoms and one half occupancy H atom, lying close to the two-fold axis. The latter H-bonds to the symmetry equivalent water oxygen (O6A) generated by the two-fold axis generating an $[H_2O_5]^+$ unit with a slightly disordered central H atom. Thus, throughout the crystal structure there are complex anion units of $[\Delta\text{-}Mo(R,R\text{-hipda})_2]^-$ linked by $[H_2O_5]^+$ units. The *R*,*R*-ligand can be used as a "lock" on the structure solutions since the chirality of the ligand is carried directly through to the complex.[29] The Mo atom sits on a crystallographic $C_2$ axis in the lattice, so the corresponding Mo–O and Mo–N bond lengths are identical within the two ligands and of a similar length to those in $[\Delta\text{-}Mo(R,R\text{-hidpa})(R,S\text{-hidpa})]^-$ [14] (Table 2), with each slightly longer (range 0.12–0.03 Å; av. 0.07 Å) than their conuterparts in $[\Delta\text{-}V(S,S\text{-hidpa})_2]^-$.[10] The planes of the two {MoNO} groups are close to perpendicular (90.2°) and effectively perpendicular (91.2 and 91.2°) to the "equatorial" plane, with significant displacements for O(1) and O(3) (−0.43 and −0.36 Å, respectively).

**3b** crystallised in the space group *Fddd* (no. 70), with the eight-co-ordinate geometry of Amavadin (Fig. 3).[5] The asymmetric unit contains half of the anion with the Mo atom located on a two-fold axis. This anion was refined as the Δ-helical form at the molybdenum(v) centre and the Λ-form is generated by the symmetry of the unit cell. The ligand was refined in exclusively the *R*,*S*-chiral form. The asymmetric unit also contains half a sodium counter cation located on a two-fold axis. Two "solvent atoms" were found disordered over two sites each, probably arising from $^iPr_2O$; it is not clear which atom is carbon and which is oxygen. As in **2**, the Mo atom sits on a crystallographic $C_2$ axis in the lattice and corresponding Mo–O and Mo–N bond lengths are identical in the two ligands. The planes of the two {MoNO} groups are not mutually perpendicular (96.5°),[30] but are effectively perpendicular (88.9, 91.1°)[30] to the equatorial plane. These oxygen atoms are significantly displaced from this plane, as found in **1** and **2**; O(1) and O(5) sit above (0.41 and 0.34 Å, respectively),[30] with the two symmetry equivalent O atoms correspondingly below, as also in **2**. The two ethyl groups of the anion of **3b** are arranged in an eclipsed fashion, this is in contrast to the staggered arrangement of these groups in the $Ta^V$ analogue[31] and both eclipsed and staggered arrangements in the $V^{IV}$ analogue,[15] although there is some disorder in the lattice water molecules.

**Table 3** Comparison of UV/vis absorption bands for **1**, **2**, **3a**, **3b** and [Δ-$PPh_4$][Mo(*R*,*R*-hidpa)(*R*,*S*-hidpa)][14]

| Compound | Solvent | $\nu$/cm$^{-1}$ | $\varepsilon$/mol$^{-1}$ dm$^{-3}$ cm$^{-1}$ |
|---|---|---|---|
| **1** | MeCN | 18181 | 19 |
| | | 26455 | 103 |
| | $CH_2Cl_2$ | 17023 | 47 |
| | | 26774 | 134 |
| **2** | $H_2O$ | 18181 | 15 |
| | | 26041 | 61 |
| **3a** | MeCN | 17730 | 10 |
| | | 26595 | 94 |
| **3b** | $H_2O$ | 17841 | 13 |
| | | 24943 | 61 |
| [$PPh_4$][Δ-Mo(*R*,*R*-hidpa)-(*R*,*S*-hidpa)] | MeCN | 18181 | 18 |
| | | 25974 | 89 |

Amavadin and its analogues crystallise with metal counter cations such as calcium and uranyl.[5,15,32,33] The sodium cation in **3b** binds to two O(2) atoms and two O(4) atoms of the carboxylate groups from four different molybdenum-containing anions. The four oxygens are arranged around the sodium in an approximately tetrahedral manner, generating an infinite lattice; the bond lengths are 2.269(7) and 2.229(7) Å for Na–O(2) and Na–O(4), respectively, and the O–Na–O inter-bond angles range from 104.6(4)–110.8(4)°.

In each case the $\eta^2$-NO groups subtend angles at the molybdenum, see Table 2, which compare with the range 39.9–41.2° observed for related vanadium systems.[9,11] The N–O bond lengths within these groups show a modest contraction from **1** to **3a** (Table 2), this correlates with an increase in the observed $\nu_{N-O}$ stretching frequency from 1108 to 1131 cm$^{-1}$. For **1**, **2** and **3b** the ligating carboxylate oxygen atoms from the same ligand are mutually *trans* and occupy sites on the same side of the least-squares plane defined by the molybdenum and the four oxygen atoms; this leads to an alternating up-down pattern of these oxygen atoms with respect to the least-squares plane.

### UV/Vis absorption spectra

Each compound has a brown–purple colour in solution and the electronic absorption spectra obtained for complexes **1**, **2** and **3a** showed a broad, low intensity, band centred at around $\nu$ = 18000 cm$^{-1}$ ($\varepsilon$ = 10–47 mol$^{-1}$ dm$^3$ cm$^{-1}$) and a more dominant feature was a medium intensity band at around $\nu$ = 26000 cm$^{-1}$ ($\varepsilon$ = 60–134 mol$^{-1}$ dm$^3$ cm$^{-1}$) (Table 3). These spectra closely resemble the UV/vis spectrum obtained for [$PPh_4$][Δ-Mo(*R*,*R*-hidpa)(*R*,*S*-hidpa)].[13] By analogy with the electronic structure proposed for Amavadin and related systems from discrete variational (DV) Xα calculations,[34] these transitions are assigned as $d_{x^2-y^2} \longrightarrow d_{yz}$, $d_{xz}$ and $d_{x^2-y^2} \longrightarrow d_{xy}$, respectively. This interpretation suggests an "electronic equivalence" between two mutually *trans* and perpendicular $\eta^2$-NO groups and one terminal oxo group.[34] The transition $d_{x^2-y^2} \longrightarrow d_{xy}$ in [M(hidca)$_2$]$^{n-}$ (where M = V, $n$ = 2 and M = Mo, $n$ = 1) would be expected to be at significantly higher energy for $Mo^V$ than $V^{IV}$, as shown for the comparison of d–d transitions in $[VOCl_4]^{2-}$ and $[MoOCl_4]^-$.[35] This transition is equivalent to 10 Dq for an octahedral complex; 10 Dq increases from 3d to 4d metals (in the same oxidation state and with the same ligands) and with increasing oxidation state. However, a similar comparison does not hold for the $d_{x^2-y^2} \longrightarrow d_{yz}$, $d_{xz}$ transitions. Thus, the difference in energy between this band in $[VOCl_4]^{2-}$ and in $[MoOCl_4]^-$ [35] is significantly less than the difference of *ca.* 6000 cm$^{-1}$ observed between the equivalent bands of the $[V(hidca)_2]^{2-}$ and $[Mo(hidca)_2]^-$ anions, indicating that the "electronic equivalence" between M=O and {M–($\eta^2$-NO)$_2$} centres is qualitative but not quantitative.[34] An intense charge transfer band in the region 32000–41000 cm$^{-1}$ was also observed in $[Mo(hidca)_2]^-$ anions. The $d_{x^2-y^2} \longrightarrow d_{z^2}$ transition is presumed to be at much higher energy than the other two d–d bands, because of ligand-field effects of molybdenum,[35] and hence obscured by the intense charge transfer absorptions.

### EPR spectra

**1**, **2** and **3a** all exhibit X-band EPR spectra in frozen solutions (**2** in $H_2O$–glycerol; **1** and **3a** in $CH_2Cl_2$–toluene) at 120 K, consistent with a Mo(V), $d^1$ configuration in each case with the ligand donor atoms arranged in the eight-co-ordinate geometry found in Amavadin. The spectra are either axial (**2**) or near axial (**1**, **3a**) and are similar to the X-band spectrum reported for [$PPh_4$][Δ-Mo(*R*,*R*-hidpa)(*R*,*S*-hidpa)].[14] These EPR spectra can be simulated using the spin-Hamiltonian parameters given in Table 4, and are consistent with a $d_{x^2-y^2}$ ground state, as previously shown for the analogous V(IV) compounds.[31] Thus, like their V(IV) counterparts, the EPR spectra of these Mo(V) complexes are indicative of the presence of a strong axial ligand field, with $g_3$ significantly smaller and $A_3$ much larger than the respective $g_1$, $g_2$, $A_1$ and $A_2$ values. The single-crystal EPR spectra of [$PPh_4$][Mo(hida)$_2$] and [$Ca(H_2O)_5$][V(hida)$_2$]·$6H_2O$ doped in their Nb and Ti analogues, respectively, have been investigated at X-band, Q-band and 180 GHz.[36] In the 180 GHz spectrum of [$PPh_4$][Nb{Mo}(hida)$_2$], all three *g*-features are split into two resonances, indicating the presence of two magnetically distinct species in the sample, and is assigned to the presence of two magnetically distinct, independent molecules in the asymmetric unit of [$PPh_4$][Nb(hida)$_2$]. These molecules have similar bond lengths and inter-bond angles. However, the dihedral angle between the two Nb–$\eta^2$-NO groups is significantly different in the two molecules (98.3 and 95.1°). The presence of two different sets of *g*- and *A*-values is consistent with the ligand-field being dominated by the {M–($\eta^2$-NO)$_2$} group and hence the *g*- and *A*-values being sensitive to variations in the geometric parameters of this group.

### Electrochemical studies

The redox properties of Amavadin and related systems have been explored in detail [7,15] and highlight the interaction between ligand and solvent in the observed $E_{1/2}$ values of the $V^V/V^{IV}$ couple. [$PPh_4$][Δ-Mo(*R*,*R*-hidpa)(*R*,*S*-hidpa)][14] is capable of both a one-electron reversible oxidation and a one-electron reversible reduction in $CH_2Cl_2$ (Table 5). We have investigated the influence of ligand and solvent on the redox chemistry of the new eight-co-ordinate molybdenum complexes reported herein.

Fig. 4 shows the cyclic voltammograms obtained for **1** and **3a** in $CH_2Cl_2$, where each complex exhibits a reversible $Mo^{VI}/Mo^V$ redox couple, analogous to that of [$PPh_4$][Δ-Mo(*R*,*R*-hidpa)-(*R*,*S*-hidpa)].[14] As with Amavadin and its relatives [7,15] shifts of ≈100 mV are observed in the $E_{1/2}$ value of the $Mo^{VI}/Mo^V$ couple for the hida$^{3-}$, hidpa$^{3-}$ and hidba$^{3-}$ as ligands within the same solvent system. The relative increased electron donating ability of hidba$^{3-}$ in **3a** compared to hida$^{3-}$ and hidpa$^{3-}$ gives rise to the lowest $E_{1/2}$ value for the $Mo^{VI}/Mo^V$ couple in $CH_2Cl_2$. The trend in $E_{1/2}$ values reported for these oxidation processes is consistent with modest variations in the electron donating ability of the individual ligands and increased solubility in organic media (Table 5). The nature of the proligand also affects the $Mo^V/Mo^{IV}$ couple of these complexes. **1** displays a quasi-reversible [37] $Mo^V/Mo^{IV}$ redox couple, however, the equivalent process for **3a** is irreversible (Fig. 4). The $Mo^V/Mo^{IV}$ couple becomes less reversible on going from **1** to **2** to **3a**. These electron transfer processes are considered to be metal-based as in the corresponding vanadium systems.[15]

A series of CPE experiments were performed for [$PPh_4$][Mo(hidpa)$_2$][14] in $CH_2Cl_2$–[$NBu^n_4$][$BF_4$] (*ca.* 0.4 mol dm$^{-3}$). The first coulometric step involved fixing the potential at +1.2 V (*vs.* SCE) and carrying out the oxidation process, thus generating $Mo^{VI}$ by exhaustive electrolysis at 293 K. On completion the

**Table 4** EPR Parameters for **1**, **2**, **3a** and $[PPh_4][\Delta\text{-Mo}(R,R\text{-hidpa})(R,S\text{-hidpa})]$

| | $g_3$ | $g_1$ | $g_2$ | $A_3$/G | $A_1$/G | $A_2$/G |
|---|---|---|---|---|---|---|
| $[PPh_4][\Delta\text{-Mo}(R,R\text{-hidpa})(R,S\text{-hidpa})]$ [a] | 1.894 | 1.974 | 1.967 | 86.0 | 29.9 | 35.0 |
| **1** [b] | 1.893 | 1.976 | 1.969 | 85.0 | 31.0 | 35.0 |
| **2** [c] | 1.890 | 1.973 | 1.973 | 86.0 | 34.0 | 34.0 |
| **3a** [b] | 1.897 | 1.976 | 1.969 | 84.0 | 31.0 | 35.0 |

[a] Ref. 14. [b] Dichloromethane–toluene (10 : 1) solution at 100 K. [c] Water–glycerol (10 : 1) solution at 100 K.

**Table 5** $E_{1/2}$ values recorded in different solvents at a glassy carbon working electrode (*vs.* SCE) for **1**, **2**, **3a** and $[PPh_4][\Delta\text{-Mo}(R,R\text{-hidpa})(R,S\text{-hidpa})]$.[14] For each reversible couple the current peak intensity ($i_p$) obeyed a linear relationship with the square root of the scan rate (range: 20–700 mV $s^{-1}$)

| Compound | Solvent/Electrolyte | $Mo^{VI}/Mo^{V}$ $E_{1/2}$/V | $\Delta E$/mV | $i_{pa} : i_{pc}$ | $Mo^{V}/Mo^{IV}$ $E_{1/2}$/V | $\Delta E$/mV | $i_{pa} : i_{pc}$ |
|---|---|---|---|---|---|---|---|
| **1** | $CH_2Cl_2/[NBu^n_4][BF_4]$ | +0.96 [a] | 70 | 0.96 | −0.99 [c] | 80 | 1.12 |
| **2** | $H_2O/KCl$ | +0.76 [b] | — | — | — | — | — |
| | $Me_2SO/[NBu^n_4][BF_4]$ | +0.77 [a] | 70 | 0.94 | −1.13 [b] | — | — |
| **3a** | $CH_2Cl_2/[NBu^n_4][BF_4]$ | +0.77 [a] | 70 | 0.95 | −1.28 [b] | — | — |
| $[PPh_4][\Delta\text{-Mo}(R,R\text{-hidpa})(R,S\text{-hidpa})]$ [11] | $CH_2Cl_2/[NBu^n_4][BF_4]$ | +0.87 [a] | — | — | −1.12 [a] | — | — |

[a] Reversible process, the current peak intensity, $i_{pa}$ and $i_{pc}$, correlated with the square root of the scan rate. [b] Irreversible process. [c] Quasi-reversible process.

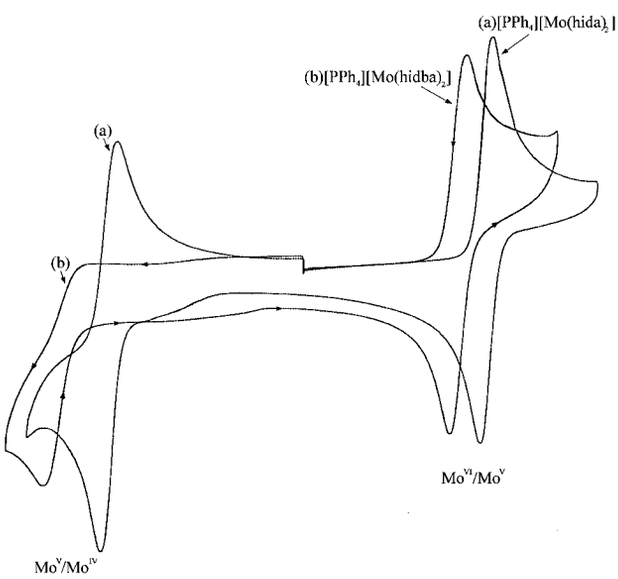


**Fig. 4** Cyclic voltammograms recorded at a glassy carbon electrode (*vs.* SCE) for **1** (a) and **3a** (b) (*ca.* 1 mmol $dm^{-3}$) in $CH_2Cl_2/[NBu^n_4][BF_4]$ (*ca.* 0.2 mol $dm^{-3}$) at 293 K, scan rate = 200 mV $s^{-1}$.

solution became pale yellow and the cyclic voltammetric experiments were repeated using a glassy carbon working electrode. The initial oxidation–reduction profiles were observed, confirming the reversibility of the $Mo^{VI}/Mo^{V}$ couple on the extended time-scale of the electrolysis experiment. A comparison of the frozen solution X-band EPR spectra before and after the electrolysis revealed a dramatic reduction in the intensity of the $Mo^{V}$ resonance, consistent with the exhaustive electrolysis achieving 95% completion of oxidation to $Mo^{VI}$. No new signal was observed in the EPR spectra, providing clear evidence that the $Mo^{VI}/Mo^{V}$ couple observed with these compounds is a metal-based one-electron transfer process. Further experiments using an OTTLE cell[22] showed distinctive changes in the UV/vis absorption spectrum of $[PPh_4][Mo(hidpa)_2]$ in $CH_2Cl_2$–$[NBu^n_4][BF_4]$ (*ca.* 0.4 mol $dm^{-3}$) upon gradual stepwise oxidation to +1.0 V (*vs.* SCE), consistent with the loss of the d–d transitions and the emergence of a charge transfer band at $\nu$ = 28000 $cm^{-1}$ ($\varepsilon$ = 790 $mol^{-1}$ $dm^{-3}$ $cm^{-1}$). The original spectrum containing the low intensity d–d absorption bands was observed after reduction of the solution at +0.5 V (*vs.* SCE). Attempts to carry out this oxidation chemically with $[NO][BF_4]$[38] yielded a pale yellow product that was only sparingly soluble in $CH_2Cl_2$ and unstable in solvents such as MeOH and $Me_2SO$ under anhydrous/anaerobic conditions.

A second exhaustive electrolysis experiment was carried out, by setting the potential to −1.5 V (*vs.* SCE), in order to produce the $[Mo(hidpa)_2]^{2-}$ moiety. This reduction step yielded a dark red solution, however, a cyclic voltammogram of this solution revealed a loss of the original sweep profile and the only feature present was an irreversible oxidation peak at +0.56 V (*vs.* SCE), consistent with an electrochemical–chemical process. This illustrates that the reduced species is not stable during the coulometric experiment and undergoes chemical reaction or rearrangement, after an initial metal-based reduction process, to produce a new product that is detected by the new oxidation peak.

Comparisons of $E_{1/2}$ values recorded for Amavadin and its relatives in $H_2O$ and $Me_2SO$ revealed shifts of ≈500 mV for equivalent redox processes,[6,17] highlighting the influence of hydrogen-bonding and other solvation effects in stabilising the oxidation state of these complexes. Fig. 5 shows the cyclic voltammograms obtained for **2** in $H_2O$ and $Me_2SO$; the $Mo^{VI}/Mo^{V}$ redox couple is reversible in $Me_2SO$ and irreversible in $H_2O$, (Table 5). This variation in the reversibility of the oxidation process, between aqueous and organic media, is in contrast to the redox chemistry of Amavadin, which displays reversible characteristics in both solvent environments,[7] and illustrates the instability of the $Mo^{VI}$, $d^0$, analogue in the presence of $H_2O$. Also in contrast to the $V^{V}/V^{IV}$ couples with $hidca^{3-}$ ligands, the difference in $E_{pa}$ between $H_2O$ and $Me_2SO$ as solvent for **2** was only *ca.* 35 mV, compared to a value of *ca.* 500 mV for the respective V complexes. A sweep to negative potentials with **2** in $H_2O$ revealed only a peak at −0.42 V (*vs.* SCE) that is due to the reduction of protons, which are present as the counter cations in **2**, and this effect was also observed for Amavadin.[7] In $Me_2SO$ the reduction process for **2** is irreversible (Table 5), highlighting again how the solvent influences the reversibility of these redox couples.

## Conclusions

The syntheses of **1**, **2**, **3a** and **3b** have further developed the chemistry of molybdenum analogues of Amavadin and X-ray crystallography has confirmed the same distinctive

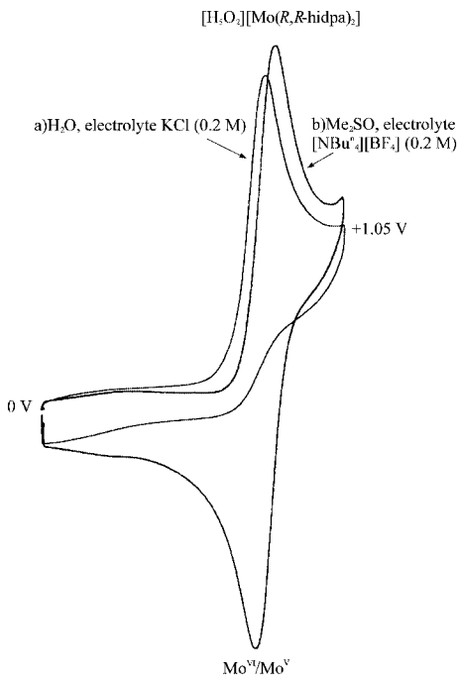


**Fig. 5** Cyclic voltammograms recorded at a glassy carbon electrode (*vs.* SCE) for **2** (a) = $H_2O$/KCl, (b) = $Me_2SO/[NBu^n_4][BF_4]$ (*ca.* 0.2 mol $dm^{-3}$) at 293 K, scan rate = 200 mV $s^{-1}$.

eight-co-ordinate geometry for the molecular anions. Cyclic voltammetry has provided a wealth of information on the redox behaviour of these molybdenum complexes and further illustrated the significant role of the solvent on the electrochemical properties of members of this family of complexes. For the molybdenum complexes the $Mo^V$, $d^1$ state is significantly preferred.

## Acknowledgements

We thank British Nuclear Fuels plc, (BNFL) for funding (to P. D. S. and S. M. H.), EPSRC for studentship funding (to J. J. A. C.) and Dr P. Harston (Company Research Laboratory, BNFL, Springfields, Preston, Lancashire) for valuable discussions during the course of this work.

## References

1 H. U. Meisch, W. Reinle and J. A. Schmitt, *Naturwissenchaften*, 1979, **66**, 620.
2 E. Bayer and H. Kneifel, *Z. Naturforsch., Teil B*, 1972, **27**, 207.
3 H. Kneifel and E. Bayer, *Angew. Chem., Int. Ed. Engl.*, 1973, **12**, 508.
4 H. Kneifel and E. Bayer, *J. Am. Chem. Soc.*, 1986, **108**, 3075.
5 R. E. Berry, E. M. Armstrong, R. L. Beddoes, D. Collison, S. N. Ertok, M. Helliwell and C. D. Garner, *Angew. Chem., Int. Ed.*, 1999, **38**, 795.
6 R. D. Gillard and R. J. Lancashire, *Phytochemistry*, 1984, **23**, 179; E. Koch, H. Kneifel and E. Bayer, *Z. Naturforsch., Teil C*, 1987, **42**, 873; P. Krauss, E. Bayer and H. Kneifel, *Z. Naturforsch., Teil B*, 1984, **39**, 829; G. Bemski, J. Felcman, J. J. R. Fraústo da Silva, I. Moura, M .C. T. A. Vaz and L. F. Vilas-Boas, *Rev. Port. Quim.*, 1985, **27**, 418; G. Bemski, J. Felcman, J. J. R. Fraústo da Silva, I. Moura, M .C. T. A. Vaz and L. F. Vilas-Boas, in *Frontiers in Bioinorganic Chemistry*, ed. A. V. Xavier, VCH, Weinheim, 1986, pp. 97–105; F. E. Mabbs, *Chem. Soc. Rev.*, 1993, **22**, 313.
7 M. A. Nawi and T. L. Riechel, *Inorg. Chim. Acta*, 1987, **136**, 33; J. J. R. Fraústo da Silva, M. F. C. G. da Silva, J. A. L. da Silva and A. J. L. Pombeiro, in *Molecular Electrochemistry of Inorganic, Bioinorganic and Organometallic Compounds*, ed. A. J. L. Pombeiro and J. A. McCleverty, Kluwer, The Netherlands, 1993, p. 411.
8 (*a*) R. D. Thackery and T. L. Reichel, *J. Electroanal. Chem.*, 1988, **245**, 131; (*b*) M. F. C. G. da Silva, J. A. L. da Silva, J. J. R. Fraústo da Silva, A. J. L. Pombeiro, C. Amatore and J.-N. Verpeaux, *J. Am. Chem. Soc.*, 1996, **118**, 7568.
9 P. M. Reis, J. A. L. Silva, J. J. R. Fraústo da Silva and A. J. L. Pombeiro, *Chem. Commun.*, 2000, 1845.
10 E. M. Armstrong, R. L. Beddoes, L. J. Calviou, J. M. Charnock, D. Collison, S. N. Ertok, J. H. Naismith and C. D. Garner, *J. Am. Chem. Soc.*, 1993, **115**, 807.
11 E. M. Armstrong, M. S. Austerberry, D. Collison, S. N. Ertok, C. D. Garner, M. Helliwell and F. E. Mabbs, unpublished work; S. N. Ertok, Ph.D. Thesis, The University of Manchester, 1993.
12 M. A. A. F. de C. T. Carrondo, M. T. L. S. Duarte, J. C. Pessoa, J. A. L. Silva, J. J. R. Fraústo da Silva, M. C. T. A. Vaz and F. L. Vilas-Boas, *J. Chem. Soc., Chem. Commun.*, 1988, 1158.
13 E. M. Armstrong, L. J. Calviou, J. M. Charnock, D. Collison, S. N. Ertok, C. D. Garner, F. E. Mabbs and J. H. Naismith, *J. Inorg. Biochem.*, 1991, **43**, 413; L. J. Calviou, Ph.D. Thesis, The University of Manchester, 1992.
14 H. S. Yadav, E. M. Armstrong, R. L. Beddoes, D. Collison and C. D. Garner, *J. Chem. Soc., Chem. Commun.*, 1994, 605.
15 P. D. Smith, R. E. Berry, S. M. Harben, R. L. Beddoes, M. Helliwell, D. Collison and C. D. Garner, *J. Chem. Soc., Dalton Trans.*, 1997, 4509.
16 P. D. Smith, S. M. Harben, R. L. Beddoes, M. Helliwell, D. Collison and C. D. Garner, *J. Chem. Soc., Dalton Trans.*, 1997, 685.
17 J. Felcman, M. Cândida, T. A. Vaz and J. J. R. Fraústo da Silva, *Inorg. Chim. Acta*, 1984, **93**, 101.
18 E. Koch, H. Kneifel and E. Bayer, *Z. Naturforsch., Teil B*, 1986, **41**, 359; G. Anderegg, E. Koch and E. Bayer, *Inorg. Chim. Acta*, 1987, **127**, 183.
19 M. M. Jones, *J. Am. Chem. Soc.*, 1959, **81**, 3188.
20 D. Collison, Ph.D. Thesis, The University of Manchester, 1979.
21 C. J. Pickett, *J. Chem. Soc., Chem. Commun.*, 1985, 323.
22 G. A. Heath, L. J. Yellowlees and P. S. Braterman, *J. Chem. Soc., Chem. Commun.*, 1981, 287.
23 R. R. Gagné, G. A. Koval and G. C. Lisensky, *Inorg. Chem.*, 1980, **19**, 2854.
24 N. Walker and D. Stewart, *Acta Crystallogr., Sect. A*, 1983, **39**, 158.
25 (*a*) G. M. Sheldrick, SHELXS-86, Program for the Solution of Crystal Structures, University of Göttingen, 1986; (*b*) P. T. Beurskens, DIRDIF, Technical Report 1984/1, Crystallography Laboratory, Toernooiveld, The Netherlands, 1984.
26 D. T. Cromer and J. T. Waber, *International Tables for X-Ray Crystallography*, The Kynoch Press, Birmingham, 1974, vol. 4, Tables 2.2A and 2.3.1.
27 (*a*) Texray Structure Analysis Package, Molecular Structure Corporation, 1985; (*b*) G. M. Sheldrick, SHELXL93, Program for the Refinement of Crystal Structures, University of Göttingen, 1993.
28 S. M. Harben, P. D. Smith, R. L. Beddoes, D. Collison and C. D. Garner, *J. Chem. Soc., Dalton Trans.*, 1997, 2777.
29 S. M. Harben, Ph.D. Thesis, The University of Manchester, 1996.
30 XPMA (version 13.8.98), L. Zsolnai, The University of Heidelberg, 1998.
31 S. M. Harben, J. J. A. Cooney, P. D. Smith, M. Helliwell, D. Collison and C. D. Garner, unpublished work.
32 S. M. Harben, P. D. Smith, R. L. Beddoes, D. Collison and C. D. Garner, *Angew. Chem., Int. Ed. Engl.*, 1997, **36**, 1897.
33 R. E. Berry, P. D. Smith, S. M. Harben, M. Helliwell, D. Collison and C. D. Garner, *Chem. Commun.*, 1998, 591.
34 E. M. Armstrong, D. Collison, R. J. Deeth and C. D. Garner, *J. Chem. Soc., Dalton Trans.*, 1995, 191.
35 D. Collison, *J. Chem. Soc., Dalton Trans.*, 1990, 2999.
36 E. J. L. McInnes, F. E. Mabbs, S. M. Harben, P. D. Smith, D. Collison, C. D. Garner, G. M. Smith and P. C. Riedi, *J. Chem. Soc., Faraday Trans.*, 1998, **94**, 3013.
37 A. J. Bard and L. R. Faulkner, *Electrochemical Methods: Fundamentals and Applications*, John Wiley & Sons, New York, 1980.
38 P. K. Ashford, P. K. Baker, N. G. Connelly, R. L. Kelly and V. A. Woodley, *J. Chem. Soc., Dalton Trans.*, 1982, 477.
39 C. K. Johnson, ORTEP, Report ORNL-5138, Oak Ridge National Laboratory, Oak Ridge, TN, 1976.